

Studies on Phenylating SBA-15 Material

QING-ZHOU ZHAI* and DONG YANG

Research Center for Nanotechnology, South Campus, Changchun University of Science and Technology, 7186 Weixing Road, Changchun 130022, P.R. China

E-mail: zhaiqingzhou@sohu.com; zhaiqingzhou@hotmail.com

Fax: (86)(431)85383815; Tel: (86)(431)85583118

Benzene (Ph) functionalized mesoporous molecular sieve of SBA-15 [Ph-(SBA-15)] was synthesized by post-synthesis method using phenyltriethoxysilane as coupling agent. The products were characterized by means of element analysis, powder X-ray diffraction, infrared spectroscopy, low-temperature nitrogen adsorption-desorption technique, transmission electron microscopy, thermogravimetry-differential thermal analysis. The results showed that phenyl was successfully grafted to the mesoporous molecular sieve SBA-15. The Ph-(SBA-15) mesoporous molecular sieve still retained the ordered mesoporous structure and possesses high thermal stability.

Key Words: Phenyltriethoxysilane, Benzene functionalization, Mesoporous molecular sieve SBA-15, Characterization.

INTRODUCTION

A molecular sieve is a material containing tiny pores of a precise and uniform size, the pore can separate or remove one substance from another on a molecular scale. Due to the very precise and uniform pore opening of the molecular sieve, certain molecules can be selectively adsorbed, while others can not. Molecular sieves have opened many new applications to the field of heterogeneous catalysis, adsorption and separation due to their large, well-defined pore sizes and high surface areas. However, for the practical applications in catalysis, these materials have been suffered from lack of active sites due to the inert nature of the silica surface. Silica surfaces in the mesoporous channels consist of siloxane (Si-O-Si) and silanol (Si-OH) groups. Chemical modification of the surface can be achieved by reaction of these groups with organosilanes containing functional groups¹⁻³. Surface functionalization of mesoporous silica has played a vital role in various technological aspects such as removal of toxic heavy metal ions from waste water⁴⁻⁶, separation⁷, purification of proteins⁸, immobilization of enzymes^{9,10}, improvement of thermal/hydrothermal stability and development of new catalysts¹¹. Various organic functional groups including thiol⁷, vinyl¹²⁻¹⁴, amine^{15,16} and propyl¹⁷ have been incorporated into the molecular sieves. SBA-15 molecular sieve is one of the largest pore size mesoporous molecular sieves with highly ordered hexagonally arranged channels,

with thick walls, adjustable pore size from 5 to 30 nm and high hydrothermal and thermal stability¹⁸. Compared to other mesoporous molecular sieves, the SBA-15 possesses larger pores, thicker walls and higher hydrothermal stability and the mesopores are interconnected by micropores¹⁹ enabling the pore surfaces to be accessed in three dimensions. The molecular sieves and its application arouse the scientist's enormous interest²⁰⁻²⁵. In the present work, benzene(Ph) functionalized mesoporous molecular sieve of SBA-15 [Ph-(SBA-15)] was synthesized by post-synthesis method using phenyltriethoxysilane as the coupling agent. Ordered large pore SBA-15 silica functionalized through one-pot synthesis was prepared.

EXPERIMENTAL

Triblock copolymer, (ethyleneglycol)-block-poly (propylenglycol)-block-poly (ethyleneglycol) (average relative molecular mass 5800, Fluka, template); tetraethyl orthosilicate (TEOS, A.R., Shanghai Chemical Ltd. Co.). Hydrochloric acid (Beijing Chemical Reagent Plant). Phenyltriethoxysilane (PTES, Zhejiang Chem-Tech Group Co. Ltd.); benzene (A.R., Tianjin Guangfu Fine Chemical Research Institute); absolute ethanol (A.R., The Second Chemical Reagent Plant of Tianjin); deionized water.

Sample preparation: The SBA-15 molecular sieve was prepared under a strong acidic condition by using triblock copolymer, poly(ethyleneglycol)-block-poly(propylene glycol)-block-poly(ethylene glycol) as the template. The procedure is as follows: 2 g of triblock copolymer, poly(ethylene glycol)-block-poly(propylene glycol)-block-poly(ethylene glycol) was dispersed in 15 g of deionized water and 60 g of HCl solution (2 mol/L) while stirring, followed by the addition of 4.25 g of tetraethyl orthosilicate to the homogeneous solution with stirring. This gel mixture was continuously stirred at 40 °C for 24 h and finally crystallized in a Teflon-lined autoclave at 100 °C for 2 d. After crystallization, the solid product was filtered, washed with deionized water and dried in air at room temperature. The material was calcined in static air at 550 °C for 24 h to decompose the triblock copolymer and a white powder (SBA-15) was obtained. This white powder was used to produce benzene (Ph) functionalized mesoporous molecular sieve [Ph-(SBA-15)] of the SBA-15 *via* the following route. First, 1.0 g of the calcined SBA-15 was placed in the mixed solution which was made up of 10 mL of benzene and 10 mL of phenyltriethoxysilane. This mixture was continuously stirred at room temperature for 72 h. The product was then filtrated and washed twice using absolute ethanol. Finally, the product was dried in air at room temperature and calcined in static air at 300 °C for 6 h to obtain the assembly product, designed as Ph-(SBA-15).

Characterization: Element analyses were performed by elementary organic microanalysis for C and H in a VERIOEL element analyzer. The content of Si was obtained by siliconantimomolybdate heteropoly blue photometry²⁶. X-ray diffraction patterns were collected with a diffractometer (D5005, Siemens, Germany) with

CuK α radiation operation at 30 kV and 20 mA for small angles (0.4°~10.0°) with step size of 0.02° and a step time of 2 s. N₂ adsorption-desorptions were carried out at 77 K on a Micromeritics ASAP2010M instrument. Before the measurements, the samples were outgassed for 12 h at 573 K. The distributions of specific surface area and pore volume with pore diameter were derived by using BET²⁷ and BJH²⁸ methods. Fourier transform infrared spectra were recorded on a Nicolet 5DX-FTIR spectrometer, using the potassium bromide wafer technique. Solid state diffuse reflectance spectra were obtained with a Cary 500 ultraviolet-visible-near infrared spectrophotometer (Varian, USA). Transmission electron microscopy (TEM) micrographs were obtained on a JEOL JEM-2000 FX electron microscope operating at 200 kV. TG-DTA experiments were performed using SDT2960 standard equipment with heating and cooling at 10 K/min in nitrogen atmospheres.

RESULTS AND DISCUSSION

The contents of the C and the H in the Ph-(SBA-15) samples are 9.86 and 1.01 %, respectively, which were determined by elemental analyzer. The content of the Si in the Ph-(SBA-15) sample was determined by siliconantimo-molybdate heteropoly blue photometry²⁶. The content of it is 21.06 %. The content of O is 68.07 % which can be calculated by that of C, H, Si. Then the molecular formula of the Ph-(SBA-15) is calculated to be C₄₁₁H₅₀₅O₂₁₂₇Si₃₇₆.

In Fig. 1, the small-angle XRD pattern of the SBA-15 (curve (a) of Fig. 1) is compared with that of the Ph-(SBA-15) (curve-b of Fig. 1). The XRD pattern of the SBA-15 shows 4 well-resolved peaks with intense diffraction peak at $2\theta = 0.88^\circ$ and 3 peaks with lower intensity at higher degree which are indexed to the 100, 110, 200 and 210 planes characteristic for highly ordered and excellent textural uniformity of a SBA-15 mesoporous material with a mesostructure of hexagonal space group symmetry p6mm¹⁸. The XRD peaks of the Ph-(SBA-15) are lower in intensity compared with those of SBA-15 and the fourth peak disappeared. The XRD results indicate that the Ph-(SBA-15) still possesses a long-range-ordered structure but the ordered degree of it decreases. The unit cell parameters (d_{100}) obtained from Fig. 1, is shown in Table-1.

TABLE-1
PORE STRUCTURE PARAMETERS OF THE SAMPLES

Sample	d_{100} (nm)	a_0^a (nm)	BET surface area (m ² g ⁻¹)	Pore volume ^b (cm ³ g ⁻¹)	Pore size ^c (nm)	Wall thickness ^d (nm)
SBA-15	9.56	11.04	1035.7	1.059	8.14	2.90
Ph-(SAB-15)	9.58	11.06	1000.1	0.999	6.77	4.29

^a $a_0 = \frac{2}{\sqrt{3}} d_{100}$; ^bBJH adsorption cumulative volume of pores; ^cPore size calculated from the adsorption branch; ^dWall thickness calculated by (a_0 - pore size).

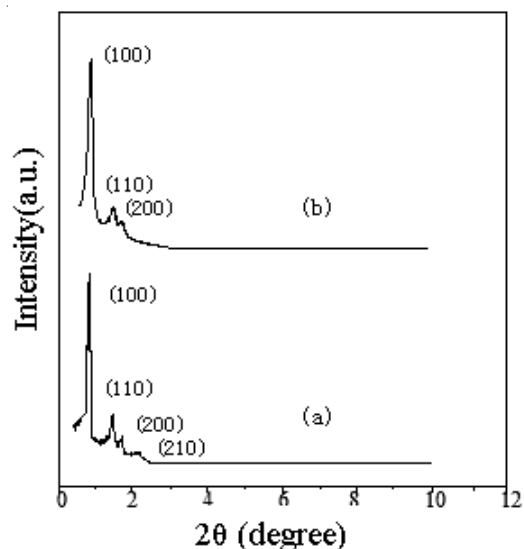


Fig. 1. XRD patterns of the samples (a) SBA-15; (b) Ph-(SBA-15)

Fig. 2 shows the FT-IR spectra of the SBA-15 and Ph-(SBA-15) samples. For the spectrum of the SBA-15 (curve-a of Fig. 2) there are several characteristic peaks. The broad band centered at 3430 cm^{-1} corresponds to that of adsorbed water. The signal at around 1092 cm^{-1} can be attributed to the asymmetric stretching vibration of the Si-O-Si. The peak present at 965 cm^{-1} is assigned to the bending vibration of the Si-OH. The peaks at 802 and 466 cm^{-1} correspond to the symmetric stretching vibration of the Si-O-Si and the bending vibration of the Si-O-Si, respectively. In curve(b) of Fig. 2 the intensity of band at 3430 cm^{-1} decreased and the band at 965 cm^{-1} disappeared. At the same time, 3 new characteristic peaks (1431 , 740 , 698 cm^{-1}) appear. The bands at 740 and 698 cm^{-1} can be attributed to the bending vibration of the C-H replaced by benzene. The band at 1431 cm^{-1} corresponds to the stretching vibration of the C-Si²⁹. The results indicate that benzene functional groups have been covalently attached to the surface of the SBA-15. Fig. 3 is the reaction schematic of the SBA-15 and phenyltriethoxysilane.

Nitrogen adsorption-desorption isotherms of the materials are shown in Fig. 4. The pore size distribution is determined by the BJH method²⁸ and the results are shown in Fig. 5. The textural data of the SBA-15 and Ph-(SBA-15) are summarized in Table-1. It can be seen from Fig. 4 that two isotherms can be classified as typical type IV according to IUPAC nomenclature²⁸. The hysteresis loop of the SBA-15 (curve-a of Fig. 4) occurs at higher relative pressure and displays a steeper capillary step, revealing that it possesses a larger pore size and a narrower pore size distribution. This can be further confirmed by the pore size distribution curve in Fig. 5(a) with a narrow peak. For the Ph-(SBA-15) a wide hysteresis loop beginning at a low relative pressure exhibits, indicating a relative wide pore size distribution and a smaller

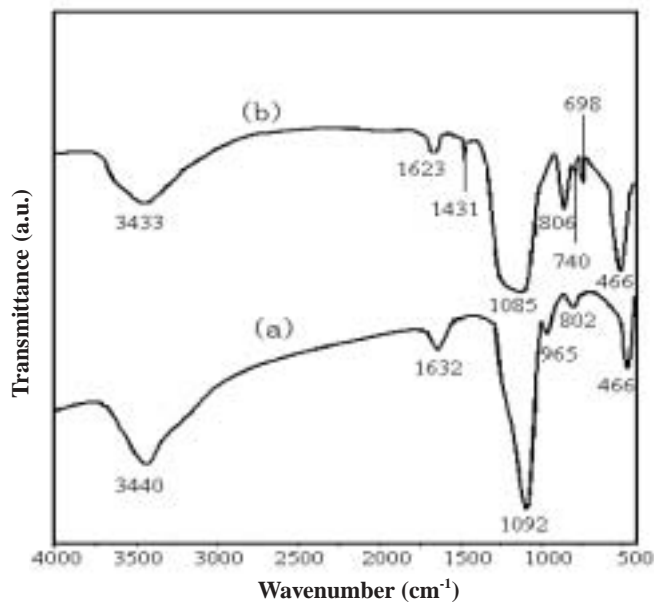


Fig. 2. Infrared spectra of the samples (a) SBA-15; (b) Ph-(SBA-15)

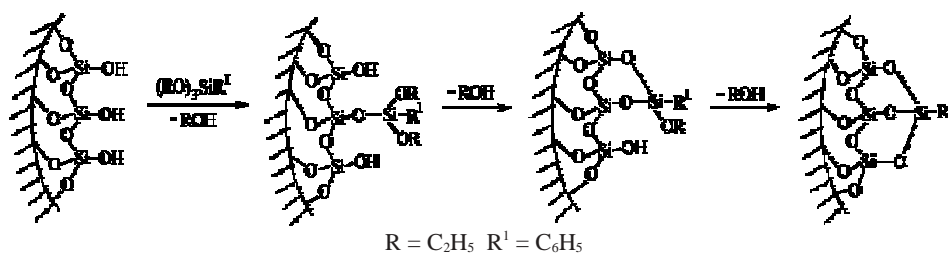


Fig. 3. Reaction schematic of the SBA-15 and phenyltriethoxysilane

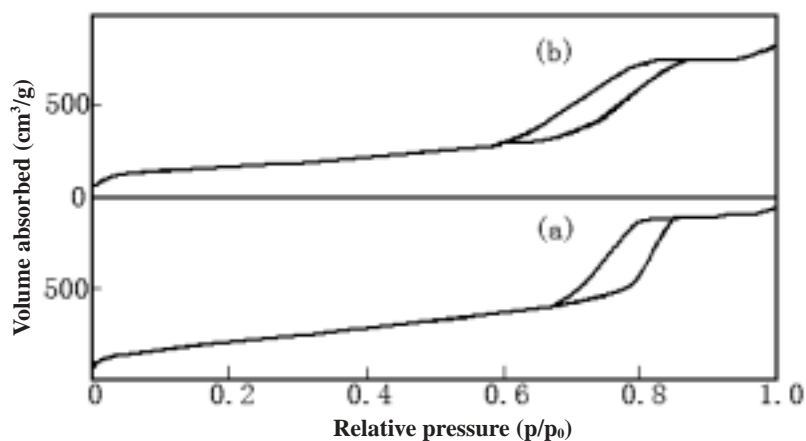


Fig. 4. Low temperature nitrogen adsorption-desorption isotherms of the samples (a) SBA-15; (b) Ph-(SBA-15)

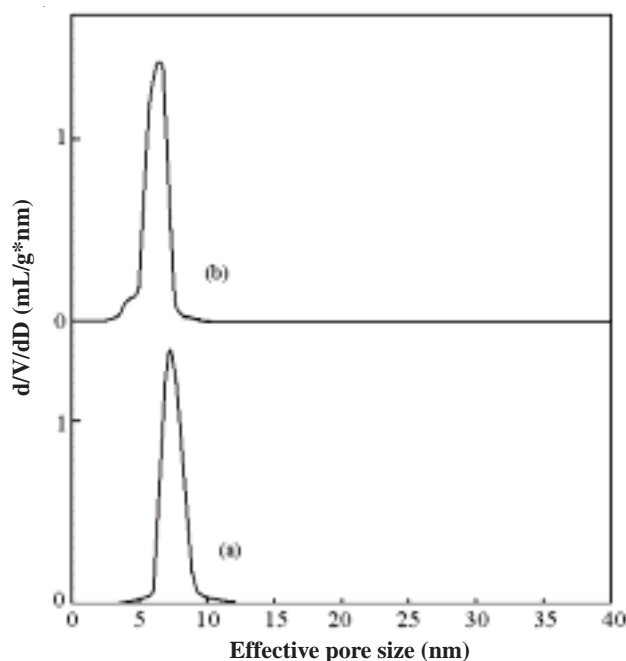


Fig. 5. Pore size distribution patterns of the samples (a) SBA-15; (b) Ph-(SBA-15)

pore diameter, as shown in Fig. 5(b). The incorporation of phenyls diminishes the pore size. Nitrogen adsorption-desorption isotherms, the pore size distribution and textural properties of the samples indicate that all samples have mesoporous channels and narrow pore size distributions and the benzene functional groups have been attached to the surface of the SBA-15.

Fig. 6 shows the TEM images of the Ph-(SBA-15). It can be seen that there is no significant collapse of the pore structure of the Ph-(SBA-15). The pore diameter (6.8 nm) measured from TEM image is in good agreement with that determined from the nitrogen adsorption. It indicates that the preparation of the sample is successful but the ordered characteristic structure of the Ph-(SBA-15) is decreased.

Fig. 7 is the TG-DTA patterns of Ph-(SBA-15). The TG curve of the Ph-(SBA-15) displays a weight loss of 1.40 % in the region of 25 to 160 °C caused by adsorbed water. Accordingly, the DTA curve exhibits a small endothermic peak at 135 °C. In the temperature range of 160-468 °C, the silanol groups of the Ph-(SBA-15) are combined with each other, losing hydroxyl group. Thus, the TG curve shows 1.97 % weight loss. In the temperature range of 468-657 °C the TG curve shows noticeable weight loss of 10.89 %, which is due to the break of the C-Si of Si-C₆H₅. Phenyl oxidation releases heat and thus the DTA curve possesses a strong exothermic peak at 600 °C. This provides that phenyl was successfully grafted to the mesoporous material. From 657 to 1000 °C the weight of samples is constant, but at 950 °C a

small peak appears in the DTA curve. This can be explained as the collapse of framework of the sample. The TG-DTA patterns suggest that the Ph-(SBA-15) possesses good thermostability.

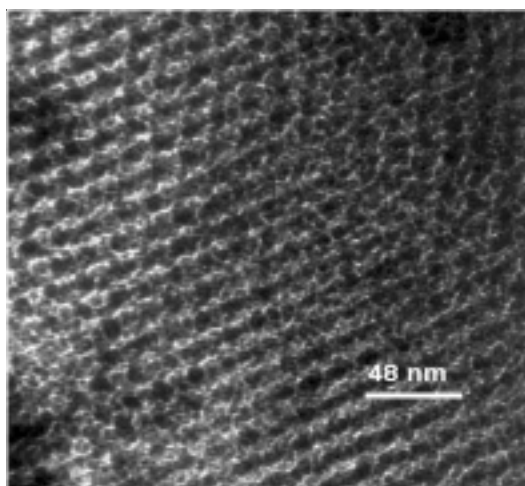


Fig. 6. TEM images of the Ph-(SBA-15) sample

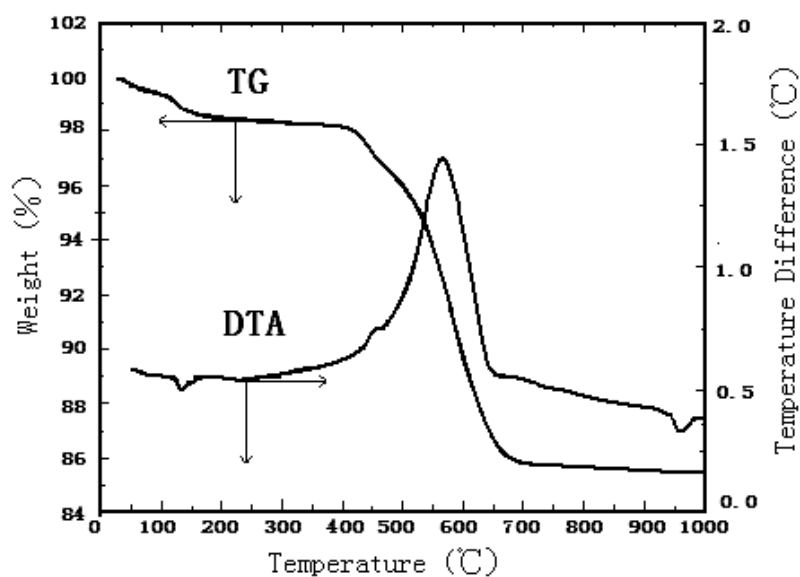


Fig.7 TG-DTA curves of the Ph-(SBA-15) sample

Conclusion

The benzene functionalized mesoporous molecular sieve of SBA-15 [Ph-(SBA-15)] was synthesized by post-synthesis method and was characterized by different techniques. Powder X-ray diffraction and transmission electron microscopy provide

evidence for the structural integrity of the benzene-functionalized SBA-15. The synthesized materials were also characterized by low-temperature nitrogen adsorption-desorption studies, indicating that all samples have mesoporous channels and a narrow pore size distributions and the benzene functional groups have been attached to the surface of the SBA-15. FT-IR studies showed that phenyl was successfully grafted to the mesoporous molecular sieve SBA-15. Thermogravimetry-differential thermal analysis technique suggested that the Ph-(SBA-15) possesses high thermal stability.

REFERENCES

1. D. Coutinho, S. Madhugiri and J.K. Balkus Jr., *J. Porous Mater.*, **11**, 239 (2004).
2. A. Sayari and S. Hamoudi, *Chem. Mater.*, **13**, 3151 (2001).
3. L. Mercier and T.J. Pinnavaia, *Chem. Mater.*, **12**, 188 (2000).
4. A.M. Liu, K. Hidajat, S. Kawi and D.Y. Zhao, *Chem. Commun.*, **13**, 1145 (2000).
5. X. Feng, G.E. Fryxell, L.Q. Wang, A.Y. Kim, J. Liu and K.M. Kemner, *Science*, **276**, 923 (1997).
6. R.J.P. Corriu, A. Mehdi, C. Reye and C. Thieuleux, *Chem. Mater.*, **16**, 159 (2004).
7. L.M. Yang, Y.J. Wang, G.S. Luo and Y.Y. Dai, *Micropor. Mesopor. Mater.*, **84**, 275 (2005).
8. Y.J. Han, G.D. Stucky and A. Butler, *J. Am. Chem. Soc.*, **121**, 9897 (1999).
9. J. Lei, J. Fan, C.Z. Yu, L.Y. Zhang, S.Y. Jiang, B. Tu and D.Y. Zhao, *Micropor. Mesopor. Mater.*, **73**, 121 (2004).
10. H.P. Yiu, P.A. Wright and N.P. Botting, *J. Mol. Catal. B*, **15**, 81 (2001).
11. A. Stein, B.J. Melde and R.C. Schrodien, *Adv. Mater.*, **12**, 1403 (2000).
12. Q. Wei, H.Q. Chen, Z.R. Nie, Y.L. Hao, Y.L. Wang, Q.Y. Li and J.X. Zou, *Mater. Lett.*, **61**, 1469 (2007).
13. H.M. Kao, J.D. Wu, C.C. Cheng and A.S.T. Chiang, *Micropor. Mesopor. Mater.*, **88**, 319 (2006).
14. N. Yu, Y. Gong, D. Wu, Y. Sun, Q. Luo, W. Liu and F. Deng, *Micropor. Mesopor. Mater.*, **72**, 25 (2004).
15. M.A. Wahab, I. Kim and C.S. Ha, *J. Solid State Chem.*, **177**, 3439 (2004).
16. Q. Wei, Z.R. Nie, Y.L. Hao, L. Liu, Z.X. Chen and J.X. Zou, *J. Sol-Gel Sci. Tech.*, **39**, 103 (2006).
17. C. Lesaint, B. Lebeau, C. Marichal and J. Patarin, *Micropor. Mesopor. Mater.*, **83**, 76 (2005).
18. D.Y. Zhao, J. Feng, Q. Huo, N. Melosh, G.H. Fredrickson, B.F. Chmelka and G.D. Stucky, *Science*, **279**, 548 (1998).
19. F. Ehrburger-Dolle, I. Morfin, E. Geissler, F. Bley, F. Livet, C. Vix-Guterl, S. Saadallah, J. Parmentier, M. Reda, J. Patarin, M. Iliescu and J. Werckmann, *Langmuir*, **19**, 4303 (2003).
20. M.H. Huang, A. Choudrey and P.D. Yang, *Chem. Commun.*, **12**, 1063 (2000).
21. Y. Han, J.M. Kim and G.D. Stucky, *Chem. Mater.*, **12**, 2068 (2000).
22. K.W. Gallis, J.T. Araujo, K.J. Duff, J.G. Moore and C.C. Landry, *Adv. Mater.*, **11**, 1452 (1999).
23. J. He, Z.H. Song, H. Ma, L. Yang and C.X. Guo, *J. Mater. Chem.*, **16**, 4307 (2006).
24. H. Friedrich, J.R.A. Sietsma, P.E. Jongh, A.J. Verkleij and K.P. Jong, *J. Am. Chem. Soc.*, **129**, 10249 (2007).
25. Q. Jiang, Z.Y. Wu, Y.M. Wang, Y. Cao, C.F. Zhou and J.H. Zhu, *J. Mater. Chem.*, **16**, 1536 (2006).
26. Q.Z. Zhai, *Hydrometallurgy of China*, **41**, 56 (1998).
27. S. Brumauer, P.H. Emmett and E. Teller, *J. Am. Chem. Soc.*, **60**, 309 (1938).
28. E.P. Barrett, L.G. Joyner and P.P. Halenda, *J. Am. Chem. Soc.*, **73**, 373 (1951).
29. K.A. Carrado, L.Q. Xu, C. Roseann and J.V. Muntean, *Chem. Mater.*, **13**, 3766 (2001).